

## HYDRODYNAMIC DRAG IN STELLER SEA LIONS (*EUMETOPIAS JUBATUS*)

LEI LANI STELLE\*, ROBERT W. BLAKE AND ANDREW W. TRITES‡

*Department of Zoology, University of British Columbia, Vancouver, British Columbia, Canada V6T 1Z4*

\*Present address: Department of Organismic Biology, Ecology and Evolution, University of California, Los Angeles, 621 Circle Drive South, Box 951606, Los Angeles, CA 90095-1606, USA (e-mail: stelle@ucla.edu)

‡Present address: Department of Zoology and Marine Mammal Research Unit, Fisheries Centre, University of British Columbia, Vancouver, British Columbia, Canada V6T 1Z4

*Accepted 27 March; published on WWW 23 May 2000*

### Summary

Drag forces acting on Steller sea lions (*Eumetopias jubatus*) were investigated from ‘deceleration during glide’ measurements. A total of 66 glides from six juvenile sea lions yielded a mean drag coefficient (referenced to total wetted surface area) of 0.0056 at a mean Reynolds number of  $5.5 \times 10^6$ . The drag values indicate that the boundary layer is largely turbulent for Steller sea lions swimming at these Reynolds numbers, which are past the point of expected transition from laminar to turbulent flow. The position of maximum thickness (at 34% of the body length measured from the tip of the nose) was more anterior than for a ‘laminar’ profile, supporting the idea that there is little laminar flow. The Steller sea lions in our study were characterized by a mean fineness ratio of 5.55. Their

streamlined shape helps to delay flow separation, reducing total drag. In addition, turbulent boundary layers are more stable than laminar ones. Thus, separation should occur further back on the animal. Steller sea lions are the largest of the otariids and swam faster than the smaller California sea lions (*Zalophus californianus*). The mean glide velocity of the individual Steller sea lions ranged from 2.9 to  $3.4 \text{ m s}^{-1}$  or 1.2–1.5 body lengths  $\text{s}^{-1}$ . These length-specific speeds are close to the optimum swim velocity of 1.4 body lengths  $\text{s}^{-1}$  based on the minimum cost of transport for California sea lions.

Key words: hydrodynamic drag, swimming, Steller sea lion, *Eumetopias jubatus*, Reynolds number, flow separation.

### Introduction

The hydrodynamic forces encountered by aquatic animals affect their energetic requirements and therefore their body morphology and swimming patterns. Steller sea lions rely on swimming to travel and forage. To move through the dense and viscous water, they must overcome a backward-acting drag force that resists forward motion. Knowledge of the magnitude of drag provides information on the flow patterns in the boundary layer adjacent to the body surface; the characteristics of this flow will influence the total cost of swimming. Pinnipeds live in both aquatic and terrestrial environments, and their body design is affected by these dual requirements. The degree of drag reduction attributable to morphological adaptations may therefore be constrained by terrestrial demands. Drag determinations allow an animal’s swimming performance, energetic requirements and body design to be assessed, thus providing insight into their ecology and behaviour.

Passive drag is the minimum drag encountered by an animal in the gliding position; drag is expected to increase during active swimming as a result of the undulatory body movements. Hydromechanic models (Lighthill, 1971; Chopra and Kambe, 1977; Yates, 1983) applied to seals and dolphins predict that power requirements should increase by two-

sevenfold compared with rigid bodies (Fish et al., 1988; Fish, 1993b). However, it has been suggested that drag is reduced in actively swimming dolphins by the formation of a negative pressure gradient along the body that stabilizes the laminar flow and damps out turbulence (Romanenko, 1995). Unlike these undulatory swimmers, sea lions swim with an essentially rigid body and move only their foreflippers to generate lift and thrust. Passive drag estimates should provide a reasonable estimate of the drag for rigid-body swimmers (Webb, 1975; Blake, 1983), such as actively swimming sea lions.

A variety of methods have been used to determine the passive drag for animals ranging from fish to large whales. All these methods require determination of the coefficient of drag ( $C_d$ ) to calculate drag. It is often assumed that a coefficient of drag can be based on a flat plate or a body of revolution with a shape similar to the study animal (Blake, 1983), but this tends to underestimate the drag and also requires assumptions about the characteristics of the boundary layer flow. Some studies have used dead animals or models to measure drag (Mordinov, 1972; Williams, 1983), but these methods have their own limitations. The body of a live animal undergoes natural deformations that may affect the drag and cannot be accounted for using this method (Williams, 1987); in addition, dead

animals often 'flutter', increasing the measured drag (Blake, 1983). Another approach, towing live animals, has the benefit of generating drag data for a large range of swimming speeds, but passive drag tends to be overestimated because animals attempt to stabilize their position with flipper movements (Feldkamp, 1987; Williams and Kooyman, 1985).

To determine accurately the minimum drag encountered by a gliding animal, video or film recordings of the 'deceleration during glide' provide the best method. This approach is based on the fact that passive glides are resisted only by the drag force of the water. The rate of deceleration can then be used to calculate the drag, employing the principle that force equals mass times acceleration. Theoretically, deceleration should occur at a constant rate, but in practice there may be small variances. Slight movements of the animal's body configuration and changes in the water current can temporarily affect the deceleration. The rate of deceleration can be determined from velocity measurements made twice, or more, over the course of the glide.

Traditionally, deceleration studies have used the 'two-point' method: velocity is measured as the animal passes two markers separated by a small distance. Bilo and Nachtigall (1980) proposed an alternative method (referred to here as the 'instantaneous rates' method); velocity is measured frequently over the course of the glide and essentially determines the instantaneous velocity. Regression of the inverse velocity against time provides a mean rate of deceleration over the entire glide, allowing the coefficient of drag to be calculated. We used this method in our study of Steller sea lions because it includes all changes in velocity, smoothes small fluctuations in the rate of deceleration, provides an assessment of whether the glide is undisturbed, and compensates for errors in measuring and plotting during the digitizing process (Bilo and Nachtigall, 1980).

The hydrodynamics of swimming for otariids has previously been investigated in only one species, the California sea lion *Zalophus californianus*. Feldkamp (1987) concluded that these sea lions have a very low drag coefficient, indicating that they maintain a partially laminar boundary layer. This is attributed in part to an optimally streamlined body form. In addition, their propulsive and aerobic efficiencies of swimming are similar to those of phocids (Williams and Kooyman, 1985; Fish et al., 1988; Williams et al., 1991) and are among the highest reported for marine mammals (Fish, 1992). Studies on California sea lions have generated valuable information, but to gain a greater understanding of otariid swimming it is necessary to study other species. Steller sea lions (*Eumetopias jubatus*) are an ideal subject. They are the largest otariid and are therefore expected to swim faster than their smaller relatives. They are also an endangered species, and information on the drag encountered during swimming can be used to model the energetic costs of swimming, an essential component of recovery plans (National Marine Fisheries Service, 1992).

Here, we investigate the passive drag of Steller sea lions over a range of natural swimming velocities. We discuss the

swimming performance of the Steller sea lions and relate it to body morphology. Their swimming performance is compared with that of other marine vertebrates, especially the closely related California sea lions. We also compare the hydrodynamic parameters from our study with predictions from the allometric relationships of Videler and Nolet (1990).

## Materials and methods

### Study animals

Six juvenile Steller sea lions (*Eumetopias jubatus* Schreber, 1776) were studied at the Vancouver Aquarium Marine Science Center in British Columbia, Canada: three females (SL2, SL3 and SL4) and three males (SL1, SL5 and SL6). The animals were held outdoors with access to both ambient sea water and haul-out areas. Their normal diet consisted of thawed herring (*Clupea harengus*) supplemented with vitamin tablets (5M26 Vitazu tablets, Purina Test Diets, Richmond, IN, USA). Glide data were collected between May 1996 and April 1997.

### Morphometrics

Morphometric measurements were collected weekly by trainers at the aquarium. Animals were weighed on a UMC 600 digital platform scale, accurate to  $\pm 0.05$  kg. Lengths and girths were measured with a tape measure while the animal was lying on cement. Maximum length ( $L$ ) was measured from nose to the end of the hindflippers, and standard length from nose to tip of tail. The fineness ratio was calculated as the maximum length divided by the diameter of the maximum girth. The position of maximum thickness ( $C$ ) was calculated as the distance from the nose to the location of maximum girth divided by maximum body length. All measurements were made for each individual at two separate times (August 1996 and March 1997) because the juvenile animals were still growing over the course of the study.

Coefficients of drag were referenced to (i.e. divided by) three different body areas: (i) total wetted surface area, (ii) frontal surface area and (iii) volume<sup>2/3</sup>. The sea lion body was treated as a series of truncated cones for calculating the reference areas. Trainers measured girths at seven places along the body: (i) the neck, (ii) directly in front of the foreflippers, (iii) directly behind the foreflippers, (iv, v) two places along the trunk region, (vi) the hips, and (vii) the position where the body and hindflippers meet. Perpendicular distances between successive girths were also measured and then adjusted to a hypotenuse length by considering the shape to be a trapezoid. The formula for the surface area of a truncated cone was applied to each of the seven increments to determine the total wetted surface area of the body core. Frontal surface area was calculated as the cross-sectional area of the body at its point of maximum width on the basis of the girth measurement made directly anterior to the foreflippers and assuming a circular shape. The surface areas of the flippers (the left foreflipper and hindflipper of each animal) were determined from images videotaped while the animal was lying face down with its

flippers extended away from the body. A measurement software program (SigmaScan/Image, version 2.01, Jandel Scientific) was used to calculate the surface area of each flipper. A reference grid in the image view was used for calibration. The surface area obtained from one side of a flipper was multiplied by two to obtain the entire flipper surface area (top and bottom), and both the left and right flippers were assumed to have the same surface area. Foreflipper span (maximum length) and maximum chord (width) were also measured from the video images. Mean chord was calculated as the surface area divided by the span. The aspect ratio was calculated as the square of the flipper's span divided by the surface area of one side. Total wetted surface area was calculated by summing the surface areas of the seven body cones and the four flippers.

Body volume was determined by calculating the volumes of the same series of cones from the girth and distance measurements. The equation for calculating the volume of the flippers (volume=span×mean chord×mean thickness) required the mean thickness of the flipper to be determined. To obtain a reasonable estimate of this varying thickness, the volume of a model made from the foreflipper of one subject was measured by water displacement. The mean thickness of this flipper was then calculated on the basis of its measured span and chord. With the assumption that thickness varied consistently with span, the relationship found for this foreflipper was then used to calculate the mean thickness of the foreflippers of the other sea lions on the basis of their own spans. The hindflippers of each individual were then assumed to have the same mean thickness as their foreflippers, and their volume was calculated using the same equation. The volume of both sets of flippers was included in the total body volume. The density of each animal was also calculated to assess the accuracy of the volume estimates. Since sea lions are thought to be neutrally buoyant (Feldkamp, 1987), their density should be close to that of the surrounding medium. The mean density ( $\pm 1$  S.D.) of the six sea lions was  $0.968 \pm 0.084 \text{ kg l}^{-1}$ , which is similar to the density of sea water,  $1.03 \text{ kg l}^{-1}$  at  $10^\circ \text{C}$  (Lide and Frederikse, 1996).

#### *Filming gliding*

Glides were recorded when the sea lions were swimming in a seawater tank measuring approximately 20 m long by 8 m wide and 3.5 m deep. Individual sea lions were filmed when they were swimming alone for positive identification of the animal. Filming was performed through a viewing window from outside the tank; the window was divided into five panels (each 110 cm wide) separated by metal columns (each 10 cm wide). The window extended higher than the water surface; the water depth viewed through the window was approximately 105 cm. A Canon ES2000 Hi-8 camcorder was set on a tripod 4.3 m from the window. The field of view included approximately half of the first window panel and all of the next three panels. Animals were filmed gliding past the window under the direction of trainers. They were directed to swim along a straight path from a rock outside the viewing area to rocks past the far right of the field of view. Although the sea

lions started the movement with a flipper stroke (outside the field of view), they glided the rest of the distance to their target. A metre stick, with visible marks delineating every 10 cm, was taped in the vertical position on the far right window divider to provide stationary reference points.

#### *Video analysis*

The Hi-8 video data were transferred to Super VHS tape with an S VHS VCR (Panasonic AG-1960); a digital counter (Panasonic) that showed elapsed time to 0.01 s was simultaneously recorded onto the tape. Individual glides were digitized on a PC with a Matrox PIP frame grabber (V software for DOS, version 1.0, Digital Optics Ltd). To evaluate the extent of parallax, a 3 m stick was placed horizontally in the water at approximately the same position as the mean glides, and a test shot was filmed. Measurements of the 10 cm intervals on the video image using the V program revealed no distortion in the field of view except at the extreme ends, which were therefore not included in the analysis of glides. The criteria used to select glides for analysis included (i) no movement of flippers and their placement near the animal's sides, (ii) no obvious horizontal movement, (iii) only gradual changes in depth (if any), and (iv) a minimum glide duration of 1 s. The sea lion's apparent maximum length was measured at the beginning, middle and end of each glide recording. These lengths (in pixels) were averaged and divided by the animal's true length (in cm) to calibrate the measurements. This method corrected for the air/water distortion and the distance of each glide from the window. Video recordings were made at  $60 \text{ frames s}^{-1}$ , and every third frame (0.05 s apart) of the video recording of the glide was used for analysis, so that there was discernible movement. Two reference points were marked on each frame to determine the distance travelled; an interval mark on the metre stick was the constant point (approximately horizontal to the glide), and the sea lion's nose acted as the moving point. When frames were skipped because the window divider blocked the reference point, missing values were filled in by linear interpolation. The measurements for each glide were then analyzed using a spreadsheet (Microsoft Excel 5.0).

The method of Bilo and Nachtigall (1980) was used to calculate the coefficient of drag ( $C_d$ ). The equation:

$$C_d = \frac{2c(M_b + M_a)}{A \times \rho}$$

requires the value of the slope of the deceleration equation ( $c$ ), the sea lion's body mass ( $M_b$ ) and the additional mass due to the entrained water ( $M_a$ ), the reference area ( $A$ ) and the density of sea water ( $\rho$ ). The most recently measured mass value for the animal and the added mass coefficient appropriate for its fineness ratio, based on an equivalent three-dimensional body of revolution (Landweber, 1961), were used in the calculations for each glide. The appropriate density and kinematic viscosity ( $\nu$ ) of sea water for the temperature on the day of the glide (Lide and Frederikse, 1996) were used in each calculation. We modified the method of Bilo and Nachtigall (1980) to reduce

scatter by applying a running average of every three analyzed frames to the measurement values. Smoothed position measurements were then subtracted to determine the distance moved between frames. These distances were divided by the time between each frame (0.05 s) to give instantaneous velocity ( $\text{m s}^{-1}$ ). A linear regression was fitted using the least-squares method to the plot of inverse velocity *versus* time. Glides were only included in the data set if the slope of the line,  $c$ , was significantly different from zero. Instantaneous velocities were averaged to describe the mean glide velocity ( $U$ ) and for calculation of Reynolds numbers ( $Re=LU/v$ ).

All statistical analyses in our study were performed using SigmaStat (for Windows, version 1.0, Jandel Scientific), and the significance level was set at  $\alpha \leq 0.05$ .

## Results

### Morphometrics

Morphometric data for each of the six sea lions (Table 1) show that all animals grew over the course of the study, with a mean weight gain of 19.2% (range 12.8–27.1%) and a mean increase in maximum length of 4.8% (range 2.2–6.7%). Morphological variables measured in the time period closest to when the glide was recorded were always used to calculate drag.

The six sea lions varied in size throughout the course of the study. The mass of the individuals ranged from 104 to 185 kg, with a maximum length of between 2.15 and 2.55 m. Total wetted surface area ranged from 2.08 to 3.03  $\text{m}^2$ , frontal surface area ranged from 0.105 to 0.194  $\text{m}^2$  and volume ranged

from 102 to 180 l. The fineness ratio was relatively consistent for all individuals over time, with a mean value of 5.55 (range 4.77–6.04). The position of maximum thickness ( $C$ ) showed minor variability, ranging from 0.307 to 0.382 with a mean of 0.344 (i.e. at 34.4% of the body length measured from the tip of the nose).

### Drag

Sixty-six glides from six individuals were analyzed to determine the drag forces. The coefficient of drag was calculated for each glide and referenced to the animal's total wetted surface area ( $C_{d,A}$ ), frontal area ( $C_{d,F}$ ) and volume<sup>2/3</sup> ( $C_{d,V}$ ). The mean values of the coefficient of drag for each animal are shown in Table 2, which also includes the mean Reynolds number, mean velocity ( $\text{m s}^{-1}$ ) and mean specific speeds (velocity converted to  $L \text{ s}^{-1}$ , where  $L$  is maximum body length).

There were no significant differences between the mean  $C_{d,A}$  values for individual sea lions (Kruskal–Wallis one-way analysis of variance, ANOVA, on ranks,  $H=6.86$ , d.f.=5,  $P=0.231$ ), so the data sets were pooled (for  $C_d$  values for all glides, see Stelle, 1997). There were significant differences between individuals in their mean  $C_{d,F}$  (one-way ANOVA,  $F=3.19$ , d.f.=5,  $P=0.0128$ ) but not in their mean  $C_{d,V}$  (Kruskal–Wallis one-way ANOVA on ranks,  $H=6.92$ , d.f.=5,  $P=0.227$ ). The coefficients of drag reveal a large amount of variability. The overall range of  $C_{d,A}$  was 0.0025–0.0098 with a mean of  $0.0056 \pm 0.0016$  (mean  $\pm 1$  s.d.).  $C_{d,V}$  ranged from 0.029 to 0.094 with a mean of  $0.053 \pm 0.016$ , and  $C_{d,F}$  ranged from 0.049 to 0.19. The  $C_{d,A}$  values appear to decrease slightly

Table 1. Morphometric data for each of the six Steller sea lions SL1–SL6

	SL1		SL2		SL3		SL4		SL5		SL6	
	Summer	Winter										
Age (years)	3	3½	3	3½	2	2½	3	3½	3	3½	3	3½
Birth year	1993		1993		1994		1993		1993		1993	
Mass (kg)	158	185	112	128	107	136	104	132	140	158	154	180
Maximum length (m)	2.23	2.37	2.28	2.33	2.27	2.33	2.15	2.27	2.25	2.40	2.42	2.55
Standard length (m)	2.01	2.06	1.88	1.95	1.90	1.97	1.81	1.92	1.99	2.03	2.05	2.08
Total wetted surface area ( $\text{m}^2$ )	2.91	3.01	2.29	2.35	2.49	2.48	2.08	2.42	2.64	2.66	2.94	3.03
Frontal surface area ( $\text{m}^2$ )	0.164	0.194	0.120	0.136	0.111	0.139	0.105	0.136	0.128	0.136	0.143	0.179
Volume (l)	173	180	119	125	136	133	102	130	151	146	178	180
Fineness ratio	4.88	4.77	5.82	5.59	6.04	5.54	5.87	5.44	5.94	5.76	5.67	5.34
Position of maximum thickness	0.359	0.350	0.382	0.343	0.379	0.313	0.307	0.343	0.351	0.329	0.347	0.325
SA of foreflippers ( $\text{m}^2$ )	0.447	0.481	0.377	0.374	0.426	0.400	0.372	0.406	0.406	0.435	0.472	0.582
Foreflipper span (m)	0.586	0.614	0.556	0.594	0.596	0.571	0.537	0.590	0.568	0.636	0.668	0.696
Mean foreflipper chord (m)	0.191	0.196	0.170	0.157	0.178	0.175	0.173	0.172	0.179	0.171	0.177	0.209
Maximum foreflipper chord (m)	0.266	0.279	0.220	0.233	0.239	0.220	0.220	0.215	0.232	0.240	0.240	0.269
Foreflipper aspect ratio	3.07	3.14	3.27	3.78	3.34	3.26	3.10	3.43	3.18	3.72	3.78	3.33

Summer measurements were taken in August 1996 and winter measurements in March 1997.

Table 2. Mean drag coefficients and associated velocities and Reynolds numbers for the six sea lions SL1–SL6

	SL1 (N=11)	SL2 (N=10)	SL3 (N=17)	SL4 (N=5)	SL5 (N=10)	SL6 (N=13)
Mean $C_{d,A}$	0.0058±0.0017	0.0046±0.00086	0.0055±0.0014	0.0074±0.0015	0.0055±0.0024	0.0055±0.0014
Mean $C_{d,F}$	0.10±0.030	0.080±0.015	0.12±0.031	0.13±0.022	0.11±0.047	0.10±0.028
Mean $C_{d,V}$	0.054±0.016	0.044±0.0080	0.052±0.013	0.070±0.014	0.053±0.023	0.052±0.013
Mean Reynolds number ( $\times 10^6$ )	5.2±0.33	5.5±0.080	5.6±0.43	5.0±0.53	5.06±0.12	6.1±0.31
Mean velocity ( $m\ s^{-1}$ )	2.9±0.19	3.4±0.049	3.2±0.17	2.9±0.33	2.9±0.071	3.2±0.26
Mean specific velocity ( $L\ s^{-1}$ )	1.3±0.084	1.5±0.021	1.5±0.081	1.3±0.13	1.2±0.030	1.3±0.070
Mean glide depth ( $H/D$ )	2.12±0.20	2.65±0.16	2.36±0.46	3.06±0.28	2.36±0.33	1.84±0.24

Values are means  $\pm$  1 s.d.

$L$ , maximum body length;  $H$ , body diameter;  $D$ , depth.

The number of glides ( $N$ ) is indicated for each sea lion.

The coefficients of drag are referenced to all three areas as follows:  $C_{d,A}$ , total wetted surface area;  $C_{d,F}$ , frontal surface area;  $C_{d,V}$ , volume<sup>2/3</sup>.

with increasing Reynolds numbers (Fig. 1), but the slope was not significantly different from zero. Theoretical drag values based on a similarly shaped spindle with a completely turbulent boundary layer are also plotted on the graph for comparison. The majority of our values lie above this predicted line and are greater by an average of 49%. Drag forces calculated from the  $C_{d,A}$  values increased with glide velocity (Fig. 2), but the relationship was not well described by the expected power regression relationship. There was a lot of

scatter around the best-fitting linear regression, with a minimum drag of 27 N and a maximum drag of 130 N. Most of the drag values for the sea lions were also greater than the theoretical values expected with a completely turbulent boundary layer by a mean of 50% (Fig. 2).

Reynolds numbers characterizing the glides ranged from  $4.6 \times 10^6$  to  $6.6 \times 10^6$ . The mean Reynolds numbers characterizing each individual's glides were significantly different between sea lions (one-way ANOVA;  $F=14.2$ , d.f.=5,  $P<0.0001$ ), but the range of the individual's means ( $5.0 \times 10^6$  to  $6.1 \times 10^6$ ) was similar to the overall range. The mean velocities

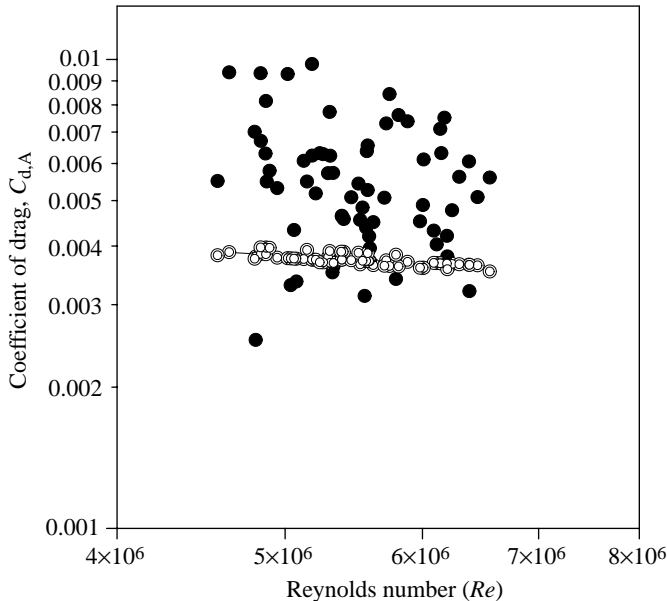


Fig. 1. Results from the glide drag experiments. The coefficients of drag referenced to the wetted surface area ( $C_{d,A}$ , filled circles) for all six Steller sea lions do not vary with the Reynolds number ( $Re$ ) of the glide. The theoretical drag for a spindle with the same fineness ratios and a completely turbulent boundary layer is indicated by the open circles. It was calculated from the equation:  $C_d = C_f [1 + 1.5(d/l)^{1.5} + 7(d/l)^3]$ , with  $C_f = 0.072 Re^{-1/5}$ , where  $C_d$  is the profile drag coefficient (sum of skin friction and pressure drag coefficients),  $C_f$  is frictional drag coefficient,  $d$  is diameter and  $l$  is length (Hoerner, 1958).

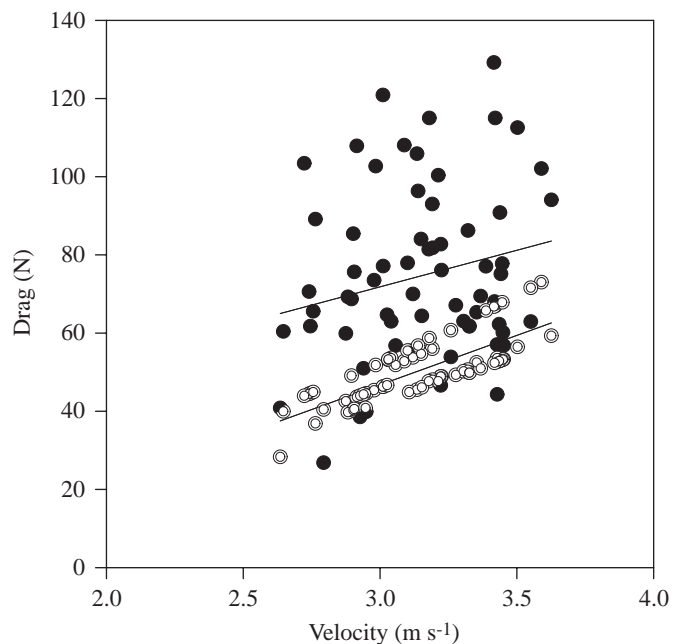


Fig. 2. Drag forces (filled circles) calculated from the  $C_{d,A}$  values (the coefficients of drag referenced to the wetted surface area) plotted against the mean velocity of the glide. The relationship for the Steller sea lions was best described by a linear regression:  $y = 15.72 + 18.7x$  ( $r^2 = 0.044$ ,  $P = 0.09$ ). The lower line represents the drag for a spindle with a turbulent boundary layer (open circles) calculated from the theoretical  $C_d$  values in Fig. 1:  $y = -29.19 + 25.32x$  ( $r^2 = 0.60$ ,  $P < 0.0001$ ).

of the glides were significantly different between individuals, both when measured in absolute terms ( $\text{m s}^{-1}$ ; one-way ANOVA,  $F=7.16$ ,  $\text{d.f.}=5$ ,  $P<0.0001$ ) and also when referenced to body length ( $L \text{ s}^{-1}$ ) (Kruskal–Wallis one-way ANOVA on ranks,  $H=32.9$ ,  $\text{d.f.}=5$ ,  $P<0.0001$ ). Mean velocities for individual sea lions ranged from 2.9 to 3.4  $\text{m s}^{-1}$  (Table 2), with an overall range of 2.6–3.6  $\text{m s}^{-1}$ . When referenced to body length, the mean specific speed for individuals was limited to 1.2–1.5  $L \text{ s}^{-1}$  (Table 2), with an overall slightly greater range of 1.1–1.6  $L \text{ s}^{-1}$ .

The depth of the filmed glides was limited because the viewing window did not extend to the bottom of the pool. The depth of the glide was reported as the number of body diameters submerged ( $H/D$ ) by measuring the distance from the water surface to the mid-point on the animal's body ( $H$ ) and dividing by the maximum body diameter ( $D$ ). The analyzed glides had depths ranging from 1.3 to 3.3  $H/D$ , with a mean depth of 2.3  $H/D$ . The coefficient of drag values appeared to be unaffected by the glide depth. The mean  $C_{d,A}$  of glides 2.7  $H/D$  and deeper was not significantly different ( $t$ -test,  $t=0.357$ ,  $\text{d.f.}=64$ ,  $P=0.722$ ) from the mean  $C_{d,A}$  of the shallower glides.

## Discussion

### Comparative drag values

Drag coefficients determined for the Steller sea lions are comparable with values obtained for other marine species (Table 3). Although the mean  $C_{d,A}$  of the Steller sea lions of 0.0056 is higher than the minimum value reported in the

marine vertebrate literature of 0.0021 for emperor penguins (Clark and Bemis, 1979), it is much lower than the value of 0.012 for bottle-nosed dolphins (Videler and Kamermans, 1985) at Reynolds numbers of approximately  $10^6$ . The mean  $C_{d,A}$  for the Steller sea lions of 0.0056 at an  $Re$  of  $5.5 \times 10^6$  is only slightly higher than the mean  $C_{d,A}$  of 0.0042 at an  $Re$  of  $2.0 \times 10^6$  reported by Feldkamp (1987) for California sea lions. The drag coefficients of Steller sea lions, and for most other marine mammals, are not substantially higher than the theoretical values for a streamlined body (Fish, 1993a). Ideal streamlined shapes, upon which the theoretical values are based, are not hindered by natural protuberances or body movements, suggesting that the animals actually have quite low drag coefficients. The measured drag coefficients show considerable variability (Fig. 1). This natural variability may reflect slight differences in body configuration during glides or changing water currents generated in the tank by their swimming. Since similar factors can affect the movements of free-ranging animals, it is important to acknowledge that the energetic costs of overcoming drag will also vary with changing conditions for animals swimming in the wild.

### Turbulent boundary layers

The majority of the drag coefficients measured in our study were greater than the theoretical values expected for a completely turbulent boundary layer, indicating that the flow on the Steller sea lions is largely turbulent. California sea lions are the only other otariid for which drag has been investigated, and Feldkamp (1987) concluded that they are able to maintain a partially laminar boundary layer. Boundary layer flow is

Table 3. Drag coefficients determined from glides for a variety of marine animals

Species	Mass (kg)	Velocity		$Re$	$C_{d,A}$	$C_{d,F}$	$C_{d,v}$	Method (glide drag)	Source
		( $\text{m s}^{-1}$ )	( $L \text{ s}^{-1}$ )						
Steller sea lion ( <i>Eumetopias jubatus</i> )	128	3.41	1.46	$5.52 \times 10^6$	0.0046	0.080	0.044	Deceleration: instantaneous rates	This study
California sea lion ( <i>Zalophus californianus</i> )	37.5	2.36	1.62	$2.87 \times 10^6$	0.0039	0.046	0.032*	Deceleration: two points	Feldkamp (1987)
Harbor seal ( <i>Phoca vitulina</i> )	33	1.8	1.4*	$1.6 \times 10^6$	0.004	0.038	NR	Deceleration: two points	Williams and Kooyman (1985)
Bottle-nosed dolphin ( <i>Tursiops truncatus</i> )	232	1.89	0.76*	$\approx 10^6$	0.012	NR	NR	Deceleration: average rate	Videler and Kamermans (1985)
Estuary dolphin ( <i>Sotalia guianensis</i> )	85	2.45	0.98*	$\approx 10^6$	0.004	NR	NR	Deceleration: average rate	Videler and Kamermans (1985)
Gentoo penguin ( <i>Pygoscelis papua</i> )	5	NR	NR	$\approx 10^6$	0.0044	0.07	0.031	Deceleration: instantaneous rates	Bilo and Nachtigall (1980)
Emperor penguins ( <i>Aptenodytes forsteri</i> )	30	1.63	1.72*	$1.25 \times 10^6$	0.0021	NR	NR	Deceleration: average rate	Clark and Bemis (1979)

$L$ , maximum body length.

If more than one value was provided for a species, the minimum  $C_d$  (of the individuals' averages) is listed, along with the associated velocity and Reynolds number ( $Re$ ).

$C_{d,A}$ , coefficient of drag referenced to total wetted surface area;  $C_{d,F}$ , to frontal surface area;  $C_{d,v}$ , to volume<sup>2/3</sup>.

Asterisks indicate values calculated from information provided; NR, not provided.

expected to be laminar for a streamlined body at an  $Re$  up to  $5 \times 10^5$ , turbulent above  $Re$  of  $5 \times 10^6$ , and transitional between these values (Blake, 1983). In our study, the Steller sea lions were swimming at Reynolds numbers ( $Re > 4 \times 10^6$ ) at which turbulence would be expected, while in the study of Feldkamp (1987) the California sea lions were swimming at  $Re < 5 \times 10^6$ , which is in the transition region. Therefore, the drag coefficients for both studies are within the predicted range on the basis of expected flow conditions in the boundary layers.

Drag coefficients vary with Reynolds number, gradually decreasing with increasing Reynolds number, dropping dramatically in the transition region, and then stabilizing in the region of turbulent flow (Blake, 1983). The  $C_{d,A}$  values of the Steller sea lions were relatively constant over the Reynolds number range of our study (Fig. 1), providing further evidence that the animals were swimming with turbulent boundary layers. Theoretically, the drag values should show a slight decrease with Reynolds number in this range. The expected slope is very small, however, which would make it difficult to demonstrate this relationship statistically using measured values. If the Steller sea lions had been swimming with a transitional boundary layer, the drastic decrease in drag should have been obvious even with the amount of variance in these measured values. Many marine mammals do swim at Reynolds numbers in the transition region, but other studies on pinnipeds and cetaceans (e.g. Innes, 1984; Videler and Kamermans, 1985; Williams and Kooyman, 1985) have also indicated that they swim with a largely turbulent boundary layer at similar Reynolds numbers ( $> 10^6$ ).

Turbulent boundary layers are associated with higher frictional drag forces than laminar ones, but have the advantage of delaying the point of separation (Vogel, 1981; Blake, 1983). Separation of flow results in a dramatic increase in pressure drag and unsteadiness in the flow that can cause buffeting of the body (Blake, 1983). Therefore, the total drag for a separated boundary layer is lower with turbulent flow than with laminar flow (Webb, 1975). Flow visualization studies on seals and dolphins have shown that the flow can remain attached along almost the entire body length (Williams and Kooyman, 1985; Rohr et al., 1998). Much less energy is then lost to wake formation, greatly reducing total drag. Yet, partially laminar flow is associated with the lowest drag forces for separated boundary layers.

It is possible that, if the Steller sea lions were to swim at slower speeds (e.g. velocity  $\approx 2 \text{ m s}^{-1}$ ,  $Re < 4 \times 10^6$ ), the lower Reynolds numbers might allow laminar flow along the anterior portion of the animal's body to be maintained. At the higher Reynolds numbers, however, laminar flow would be difficult to maintain without separation. Therefore, it is likely that, at the mean swimming speeds of Steller sea lions, the boundary layer is turbulent, separation of the flow is delayed and the total drag is reduced compared with a separated laminar boundary layer. The results from our study agree with other research on marine mammal swimming (Lang and Pryor, 1966; Fish et al., 1988; Fish, 1993b) that show no unusual ability to maintain laminar flow as was once proposed by Gray (1936).

Drag is proportional to the square of velocity and should therefore increase curvilinearly with swimming velocity. In our study, drag actually had more of a linear response (Fig. 2). The drag values were greater than the minimum theoretical values for a completely turbulent boundary layer but showed the same linear trend. This can be attributed to the limited range of swimming velocities over which drag was measured. If a broader range of velocities had been investigated, the drag would be expected to show a curvilinear response similar to that found for California sea lions (Feldkamp, 1987) and harbor seals (Williams and Kooyman, 1985).

Swim studies in enclosed tanks are not exact simulations of free swimming in the wild because of wave interference with the walls, shallow depths and restricted distances. It is predicted that an animal swimming near the surface of the water will encounter additional drag forces from the formation of wave drag (Hertel, 1966). In theory, this drag augmentation is greatest at a depth of 0.5 body diameters, and the effect decreases until it is negligible at 3 body diameters below the surface. An experimental study on harbor seals and humans showed the expected increase in drag when the subjects were towed at the surface compared with submerged tows (Williams and Kooyman, 1985). Yet, in our study on Steller sea lions, there was no apparent effect of depth on the drag coefficients. This is probably because our animals were entirely submerged, with a mean glide depth of  $2.3H/D$ . The expected augmentation in this region is small (Hertel, 1966). Although the glides appear to have been sufficiently deep to reduce surface drag, there could still be other influences on the drag, such as interference with the surrounding tank walls. This effect cannot be quantified, but most glides appeared to be greater than 1 body diameter from the wall. Any increase in drag would therefore be minimal. Errors in the digitizing process and calculation of reference area are the main contributors to the total experimental error in the drag coefficients, which was estimated to be approximately 18% (Stelle, 1997). Although this may seem high, it is less than the natural variability displayed by the animals in our study.

#### *Morphological adaptations*

The streamlined body forms of most marine animals represent a prime example of convergent evolution in their design to minimize drag for locomotion in the water (Howell, 1930). At high Reynolds numbers, streamlining provides an effective means of reducing drag by delaying the point of boundary layer separation (Vogel, 1981; Blake, 1983). Fineness ratios are a measure of streamlining, and values from 2 to 6 result in reduced drag, with an optimum at 4.5 (Blake, 1983). The Steller sea lions have a streamlined body with a mean fineness ratio of 5.55, a value similar to that of other marine mammals including seals, dolphins and whales (Fish, 1993a).

The position of maximum thickness is another indicator of the magnitude of drag; larger values indicate that separation of the boundary layer occurs further back on the body surface, thus decreasing overall drag (Mordinov, 1972). Boundary layer

separation is expected to occur at this position and has been observed on a model dolphin (Purves et al., 1975). Yet, studies on freely swimming seals and dolphins show no separation of the flow until near the end of the body (Williams and Kooyman, 1985; Rohr et al., 1998). The position of maximum thickness ( $C$ ) is also important because it is often the point where boundary layer flow switches from laminar to turbulent (Vogel, 1981; Blake, 1983). Placement of this position further posterior allows a greater region of laminar flow and therefore lower overall drag. The Steller sea lions in our study had a mean  $C$  of 0.34 (range 0.31–0.38). This is slightly lower than the reported values of 0.40 for California sea lions (Feldkamp, 1987) and 0.34–0.45 for dolphins (Fish and Hui, 1991) and much lower than the range of 0.5–0.6 for phocid seals (Aleyev, 1977; Innes, 1984). The position of maximum thickness on otariids coincides with the location of their shoulders and foreflippers. This location may be constrained by their evolutionary history (Lauder, 1982) and may also be associated with the demands of terrestrial locomotion, which relies on the foreflippers for quadrupedal movement.

The large surface area of the foreflippers of the Steller sea lion constitute approximately 16.5% of their total wetted body surface area, a proportion almost identical to the mean value of 16.2% for California sea lion foreflippers (Feldkamp, 1987). The mean aspect ratio of the flippers of the Steller sea lions was 3.37, which is substantially lower than the mean value of 7.85 measured for California sea lions (Feldkamp, 1987). The aspect ratio of the foreflipper of the Steller sea lion is also low in comparison with that of bird and insect wings (Vogel, 1981). The foreflippers of Steller sea lions are large and long, like an ideal hydrofoil, but they are also rather wide, which reduces the aspect ratio.

#### *Swimming velocities*

Our experimental design allowed the animals to swim at the speed of their choice. This limited the range of drag data, but provided an opportunity to evaluate their preferred swimming speeds. These speeds are likely to vary in the wild, but results from our study give an indication of the velocities at which Steller sea lions swim. The mean glide velocities of individuals ranged from 2.9 to 3.4  $\text{m s}^{-1}$ ; these values are higher than the mean value of 2.0–2.4  $\text{m s}^{-1}$  for California sea lions (Feldkamp, 1987). It is expected that Steller sea lions should swim faster than their smaller relatives because, although drag increases with the square of velocity, the available power increases with the cube of the body length (Aleyev, 1977). However, when glide velocity is referenced to body length (specific speed;  $L \text{ s}^{-1}$ ), the mean specific speeds for the Steller sea lions of 1.2–1.5  $L \text{ s}^{-1}$  are lower than those measured for the California sea lions of 1.6–1.8  $L \text{ s}^{-1}$  (Feldkamp, 1987). This reduction in specific speed for larger animals has also been observed in cetaceans (Webb, 1975; Fish, 1998).

The minimum cost of transport (COT) is the amount of energy required to move a unit of mass a given distance (Schmidt-Nielsen, 1972) and predicts the velocity at which the greatest distance can be travelled with the least energetic costs.

The preferred swimming speed should therefore match the speed of minimum COT. This has been demonstrated in animals ranging from ducks (Prange and Schmidt-Nielsen, 1970) to sea lions (Feldkamp, 1985). Feldkamp (1987) determined that the minimum COT occurred at 1.8  $\text{m s}^{-1}$  or 1.4  $L \text{ s}^{-1}$  for California sea lions, a specific speed identical to the overall mean for the Steller sea lions in our study. Ponganis et al. (1990) recorded the velocities of otariids in the wild and showed that the mean speeds of the smaller species were consistent with predictions based on the minimum COT (Feldkamp, 1987), while the larger animals tended to swim more slowly than expected.

Videler and Nolet (1990) compared the costs of swimming in 39 species (nine surface swimmers and 30 submerged swimmers) and developed predictive relationships based on the compiled data. The mean optimum swimming speed ( $u_{\text{opt}}$ , e.g. minimum COT) for all 39 species was 1.54  $L \text{ s}^{-1}$ , a value similar to the overall mean specific swimming speed displayed by the Steller sea lions of 1.4  $L \text{ s}^{-1}$ . The regression of Videler and Nolet (1990),  $u_{\text{opt}} = 0.002 Re^{0.48}$  (where  $u_{\text{opt}}$  is in  $\text{m s}^{-1}$ ;  $r^2 = 0.95$ ,  $N = 30$ ), predicted an optimum swimming speed of 3.4  $\text{m s}^{-1}$  on the basis of the mean Reynolds numbers from our study. This is similar to our observed mean swimming speed of 3.1  $\text{m s}^{-1}$ . The relationships based on mass  $M$  ( $u_{\text{opt}} = 0.5 M^{0.27}$  and  $Re = 2.0 E 5 M^{0.6}$ ) were much less successful in predicting  $u_{\text{opt}}$  and  $Re$ . The regressions predicted a value of 1.9  $\text{m s}^{-1}$  ( $r^2 = 0.85$ ,  $N = 30$ ), compared with the mean swimming speed of the Steller sea lions of 3.1  $\text{m s}^{-1}$ , and a Reynolds number of  $3.9 \times 10^6$  ( $r^2 = 0.95$ ,  $N = 39$ ) compared with our observed mean of  $5.5 \times 10^6$ . This discrepancy may be because Reynolds number provides a better indication of flow conditions than does body mass.

#### *Concluding remarks*

Steller sea lions utilize the same propulsion mode as other otariids, but their performance differs somewhat from California sea lions because of their larger size. As predicted, Steller sea lions reached higher swimming velocities which, together with their greater body length, resulted in higher Reynolds numbers. Gliding occurred at Reynolds numbers beyond the transition zone. It is therefore not surprising that the drag data indicated that Steller sea lions swim with a largely turbulent boundary layer. This is not necessarily a disadvantage, however, because the turbulence in the flow should delay separation of the boundary layer, resulting in a lower overall drag. Their well-streamlined bodies also help to delay separation with a near optimum fineness ratio. Steller sea lions, like other marine mammals, exhibit no unusual ability to maintain laminar flow, but still encounter relatively low drag. This information can be used to model the energetic costs of swimming and to determine the contribution of swimming costs to their overall energetic expenditures.

The authors would like to thank T. Shannon, C. Porter and D. Christen for their help in the handling and training of the sea lions and the Vancouver Aquarium Marine Science Center

for providing research facilities. We also greatly appreciate the assistance of D. Rosen, J. Gosline, W. Megill, T. Law and M. Kasapi. Comments from two anonymous reviewers improved the manuscript. This work was funded by grants to the North Pacific Universities Marine Mammal Research Consortium from the North Pacific Marine Science Foundation (A.W.T.) and a grant from the Natural Science and Engineering Research Council of Canada (R.W.B.).

### References

- Aleyev, Y. G.** (1977). *Nekton*. The Hague: Junk.
- Bilo, D. and Nachtigall, W.** (1980). A simple method to determine drag coefficients in aquatic animals. *J. Exp. Biol.* **87**, 357–359.
- Blake, R. W.** (1983). *Fish Locomotion*. London: Cambridge University Press.
- Chopra, M. G. and Kambe, T.** (1977). Hydrodynamics of lunata-tail swimming propulsion. Part 2. *J. Fluid Mech.* **9**, 49–69.
- Clark, B. D. and Bemis, W.** (1979). Kinematics of swimming of penguins at the Detroit zoo. *J. Zool., Lond.* **188**, 411–428.
- Feldkamp, S. D.** (1985). Swimming and diving in the California sea lion, *Zalophus californianus*. PhD dissertation, University of California, San Diego, USA.
- Feldkamp, S. D.** (1987). Swimming in the California sea lion: morphometrics, drag and energetics. *J. Exp. Biol.* **131**, 117–135.
- Fish, F. E.** (1992). Aquatic locomotion. In *Mammalian Energetics: Interdisciplinary Views of Metabolism and Reproduction* (ed. T. E. Tomasi and T. H. Horton), pp. 34–63. New York: Cornell University Press.
- Fish, F. E.** (1993a). Influence of hydrodynamic design and propulsive mode on mammalian swimming energetics. *Aust. J. Zool.* **42**, 79–101.
- Fish, F. E.** (1993b). Power output and propulsive efficiency of swimming bottlenose dolphins (*Tursiops truncatus*). *J. Exp. Biol.* **185**, 179–193.
- Fish, F. E.** (1998). Comparative kinematics and hydrodynamics of odontocete cetaceans: morphological and ecological correlates with swimming performance. *J. Exp. Biol.* **201**, 2867–2877.
- Fish, F. E. and Hui, C. A.** (1991). Dolphin swimming – a review. *Mammal Rev.* **B 21**, 181–195.
- Fish, F., Innes, S. and Ronald, K.** (1988). Kinematics and estimated thrust production of swimming harp and ringed seals. *J. Exp. Biol.* **137**, 157–173.
- Gray, J.** (1936). Studies in animal locomotion. VI. The propulsive powers of the dolphin. *J. Exp. Biol.* **10**, 88–104.
- Hertel, H.** (1966). *Structure, Form, Movement*. New York: Reinhold Publishing Corporation.
- Hoerner, S. F.** (1958). *Fluid-Dynamic Drag*. Midland Park, NJ: published by the author.
- Howell, A. B.** (1930). *Aquatic Mammals*. Springfield, IL: Charles C. Thomas-Publisher.
- Innes, H. S.** (1984). Swimming energetics, metabolic rates and hind limb muscle anatomy of some phocid seals. PhD dissertation, University of Guelph, Ontario.
- Landweber, L.** (1961). Motion of immersed and floating bodies. In *Handbook of Fluid Dynamics* (ed. V. L. Streeter), pp. 13-1–13-50. New York: McGraw-Hill Book Co.
- Lang, T. G. and Pryor, K.** (1966). Hydrodynamic performance of porpoises (*Stenella attenuata*). *Science* **152**, 531–533.
- Lauder, G. V.** (1982). Historical biology and the problem of design. *J. Theor. Biol.* **97**, 57–67.
- Lide, D. R. and Frederikse, H. P. R.** (1996). (eds) *CRC Handbook of Chemistry and Physics*, 77th edition. New York: CRC Press.
- Lighthill, Sir, J.** (1971). Large-amplitude elongated body theory of fish locomotion. *Proc. R. Soc. Ser. B* **179**, 125–138.
- Mordinov, Y. E.** (1972). Some hydrodynamic parameters of body shape in Pinnipedia. *Hydrobiol. J.* **8**, 81–84.
- National Marine Fisheries Service (NMFS).** (1992). *Recovery Plan for the Steller Sea Lion Eumetopias jubatus*. Silver Spring, Maryland: NMFS.
- Ponganis, P. J., Ponganis, E. P., Ponganis, K. V., Kooyman, G. L., Gentry, R. L. and Trillmich, F.** (1990). Swimming velocities in otariids. *Can. J. Zool.* **68**, 2105–2112.
- Prange, H. D. and Schmidt-Nielsen, K.** (1970). The metabolic cost of swimming in ducks. *J. Exp. Biol.* **53**, 763–777.
- Purves, P. E., Dudok Van Heel, W. H. and Jonk, A.** (1975). Locomotion in dolphins. Part I. Hydrodynamic experiments on a model of the bottle-nosed dolphin, (*Tursiops truncatus*). *Mont. Aquat. Mamm.* **3**, 5–31.
- Rohr, J., Latz, M. I., Fallon, S., Nauen, J. C. and Hendricks, E.** (1998). Experimental approaches towards interpreting dolphin-stimulated bioluminescence. *J. Exp. Biol.* **201**, 1447–1460.
- Romanenko, E. V.** (1995). Swimming of dolphins: experiments and modelling. In *Biological Fluid Dynamics* (ed. C. P. Ellington and T. J. Pedley), pp. 21–33. Cambridge: The Company of Biologists Ltd.
- Schmidt-Nielsen, K.** (1972). Locomotion: energy cost of swimming, flying and running. *Science* **177**, 222–228.
- Stelle, L. L.** (1997). Drag and energetics of swimming in Steller sea lions (*Eumetopias jubatus*). MSc thesis, University of British Columbia.
- Videler, J. and Kamermans, P.** (1985). Differences between upstroke and downstroke in swimming dolphins. *J. Exp. Biol.* **119**, 265–274.
- Videler, J. J. and Nolet, B. A.** (1990). Costs of swimming measured at optimum speed: scale effects, differences between swimming styles, taxonomic groups and submerged and surface swimming. *Comp. Biochem. Physiol. A* **97**, 91–99.
- Vogel, S.** (1981). *Life in Moving Fluids*. Boston, MA: Willard Grant Press.
- Webb, P. W.** (1975). Hydrodynamics and energetics of fish propulsion. *Bull. Fish. Res. Bd Can.* **190**, 1–159.
- Williams, T. M.** (1983). Locomotion in the North American mink, a semi-aquatic mammal. I. Swimming energetics and body drag. *J. Exp. Biol.* **103**, 155–168.
- Williams, T. M.** (1987). Approaches for the study of exercise, physiology and hydrodynamics in marine mammals. In *Approaches to Marine Mammal Energetics* (ed. A. C. Huntley, D. P. Costa, G. A. J. Worthy and M. A. Castellini), pp. 127–145. Kansas: Allen Press.
- Williams, T. M. and Kooyman, G. L.** (1985). Swimming performance and hydrodynamic characteristics of harbor seals *Phoca vitulina*. *Physiol. Zool.* **58**, 576–589.
- Williams, T. M., Kooyman, G. L. and Croll, D. A.** (1991). The effect of submergence on heart rate and oxygen consumption of swimming seals and sea lions. *J. Comp. Physiol. B* **160**, 637–644.
- Yates, G. T.** (1983). Hydromechanics of body and caudal fin propulsion. In *Fish Biomechanics* (ed. P. W. Webb and D. Weihs), pp. 177–213. New York: Praeger Publishing Co.